Electronic Supplementary Information (ESI)

Highly Efficient Deep-Blue Fluorescence OLEDs with Excellent Charge Balance Based on Phenanthro[9,10-*d*]oxazole-Anthracene Derivatives

Seokwoo Kang,[a] Jin-Suk Huh,[b] Jang-Joo Kim*[b] and Jongwook Park*[a]

[a] Department of Chemical Engineering, Kyung Hee University, Gyeonggi, 17104, Korea
[b] Department of Material Science and Engineering, Research Institute of Advanced Materials (RIAM), Seoul National University of Korea, 08826, Korea
E-mail: jjkim@snu.ac.kr (Jang-Joo Kim), jongpark@khu.ac.kr (Jongwook Park)

General information

Reagents and solvents were purchased as reagent grade and used without further purification. Analytical TLC was carried out on a Merck 60 F254 silica gel plate, and column chromatography was performed using Merck 60 silica gel (230–400 mesh). The ^{1}H-NMR spectra were recorded on Bruker Avance 300 spectrometers. The FAB+-mass and EI+-spectra were recorded on JMS-600W and JMS-700, 6890 Series mass spectrometers and Flash 1112 and Flash 2000 analyzers. The optical UV-Vis absorption spectra were obtained using a Lambda 1050 UV/Vis/NIR spectrometer (PerkinElmer). A PerkinElmer luminescence spectrometer LS55 (xenon flash tube) was used to perform PL spectroscopy. The glass transition temperatures (T_g) of the compounds were obtained using DSC under a nitrogen atmosphere using a DSC 4000 thermal analyzer (PerkinElmer). The decomposition temperatures (T_d) of the compounds were measured with TGA using a TGA 4000 thermogravimetric analyzer (PerkinElmer). The HOMO energy levels were determined with ultraviolet photoelectron yield spectroscopy (AC-2; Riken Keiki). The LUMO energy levels were derived from the HOMO energy levels and the band gaps.

- Fabrication of thin films and OLEDs

Each thin film was fabricated by thermal evaporation in a vacuum of < 5×10^{-7} Torr at a deposition rate of 1 Å sec^{-1}.

- PLQY of thin films

The PLQY of the thin films was determined using a photomultiplier tube (PMT; Acton Research Corp.) combined with an integrating sphere with a He:Cd laser as an excitation source.

- Horizontal dipole ratio

The horizontal dipole ratios of the materials were obtained by fitting the angle-dependent *p*-polarized PL measurement results with optical calculation. The detailed experimental setup is described in our previous report.[44]

- Transient PL decay profile

Transient PL decay profiles of the films were measured using a streak camera (Hamamatsu Photonics) with a pulsed N_2 laser as an excitation source (λ = 325 nm, pulse width = 700 ps; Ushio laser).

- J-V-L/EQE/CE/ADEL

The current densities of the OLEDs were measured using a source meter (Keithley 2400; Keithley). EL spectra, luminance, and current efficiencies in the normal direction of the OLEDs were measured using a spectrocolorimeter (PR650; Photo Research). The EQE values of the OLEDs were calibrated with angle-dependent EL (ADEL) spectra measurements. In the ADEL measurements, the device was automatically rotated using a rotation stage and the EL spectrum was measured using a fiber-coupled spectrometer (S2000; Ocean Optics Inc.).

- Transient EL decay profile

Transient EL decay profiles of the OLEDs were measured using a PMT combined with an oscilloscope (54642A; Agilent Technologies). Voltage pulses were applied to the OLEDs using a function/arbitrary waveform generator (33250A; Agilent Technologies). The pulse width and the frequency of the voltage pulses were 500 μs and 100 Hz, respectively. To remove the effect of trapped and accumulated charges, a base voltage of –5 V was applied.

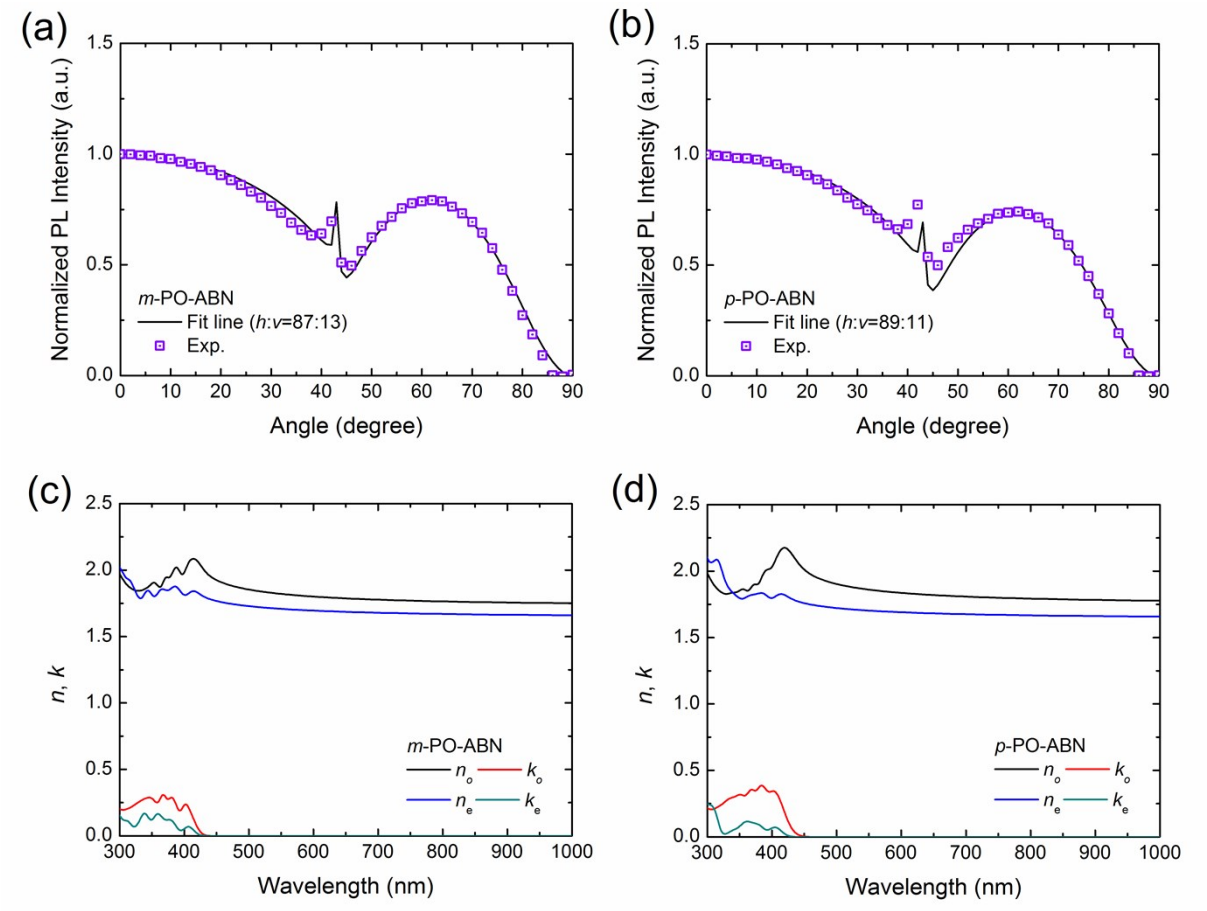

Fig. S1 Angle-dependent *p*-polarized photoluminescence intensity profiles at the peak wavelength (symbol) along with a theoretical fit line (solid line) for (a) *m*-PO-ABN and (b) *p*-PO-ABN. Anisotropic refractive indices of (c) *m*-PO-ABN and (d) *p*-PO-ABN.

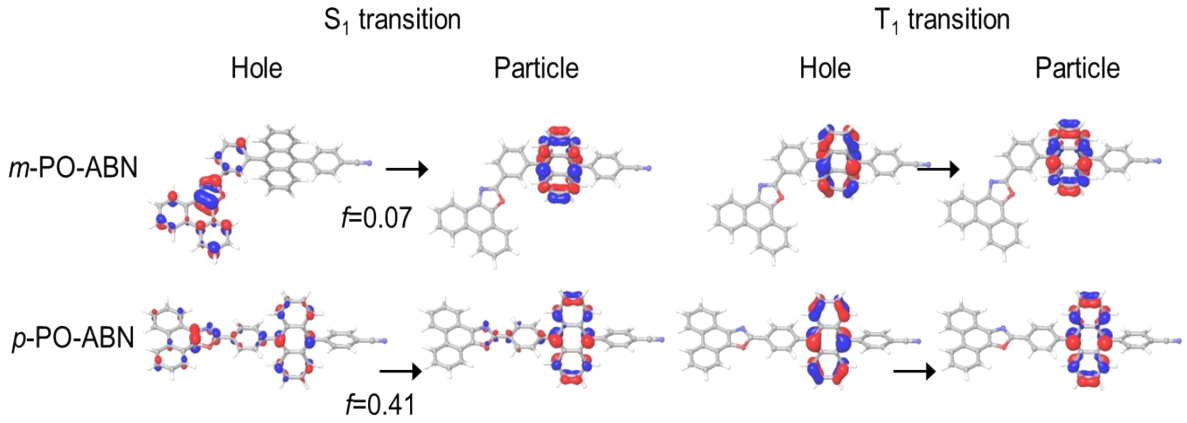

Fig. S2 Transition properties and natural transition orbitals (NTOs) of the excited state for *m*-PO-ABN and *p*-PO-ABN (calculated at the Jaguar, B3LYP/6-31G**).

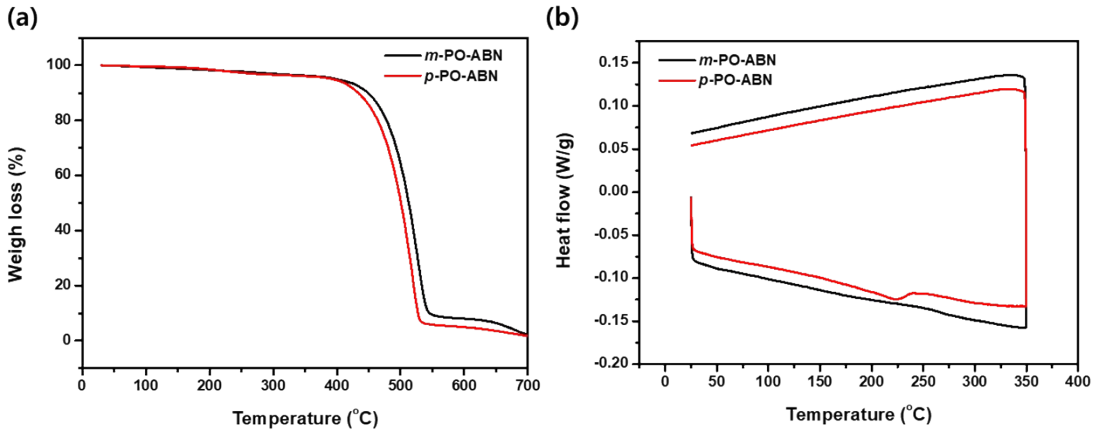

Fig. S3 (a) TGA and (b) DSC curves of the synthesized compounds.

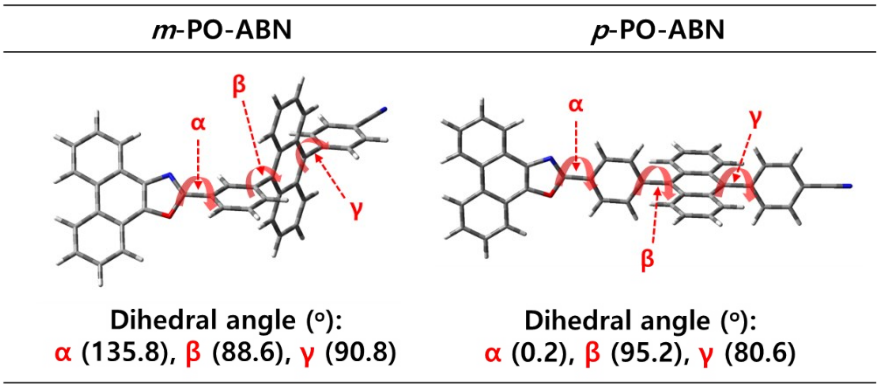

Fig. S4 Optimization structure and dihedral angles of *m*-PO-ABN and *p*-PO-ABN (calculated at the B3LYP/6-31G(d)).

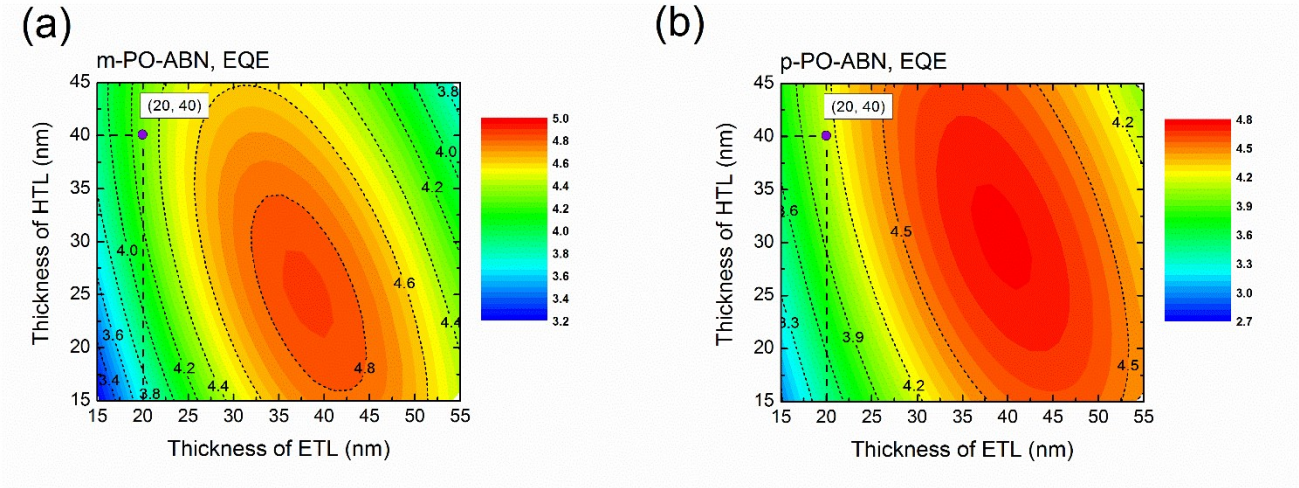

Fig. S5 Calculated achievable external quantum efficiency of the OLEDs without triplet exciton harvesting via TTA (η_{rad} = 0.25) as a function of ETL thickness and HTL thickness for (a) *m*-PO-ABN and (b) *p*-PO-ABN.